ACS OMEGA

http://pubs.acs.org/journal/acsodf

Article

Critical Properties of Ternary Deep Eutectic Solvents Using Group Contribution with Extended Lee−Kesler Mixing Rules

Abir Boublia,[▽] Tarek Lemaoui,[▽] Ghaiath Almustafa, Ahmad S. Darwish, Yacine Benguerba, Fawzi Banat, and Inas M. AlNashef*

Cite This: *ACS Omega* 2023, 8, 13177−13191

Read Online

ACCESS | Metrics & More | Article Recommendations | Supporting Information

ABSTRACT: One of the most commonly used molecular inputs for ionic liquids and deep eutectic solvents (DESs) in the literature are the critical properties and acentric factors, which can be easily determined using the modified Lydersen−Joback−Reid (LJR) method with Lee−Kesler mixing rules. However, the method used in the literature is generally applicable only to binary mixtures of DESs. Nevertheless, ternary DESs are considered to be more interesting and may provide further tailorability for developing task-specific DESs for particular applications. Therefore, in this work, a new framework for estimating the critical properties and the acentric factor of ternary DESs based on their molecular structures is presented by adjusting the framework reported in the literature with an extended version of the Lee−Kesler mixing rules. The presented framework was applied to a data set consisting of 87 ternary DESs with 334 distinct compositions. For validation, the estimated critical properties and acentric factors were used to predict the densities of the ternary DESs. The results showed excellent agreement between the experimental and calculated data, with an average absolute relative deviation (AARD) of 5.203% for ternary DESs and 5.712% for 260 binary DESs (573 compositions). The developed methodology was incorporated into a user-friendly Excel worksheet for computing the critical properties and acentric factors of any ternary or binary DES, which is provided in the Supporting Information. This work promotes the creation of robust, accessible, and user-friendly models capable of predicting the properties of new ternary DESs based on critical properties, thus saving time and resources.

1. INTRODUCTION

Since their first report in 2001,[1] deep eutectic solvents (DESs) have attracted the interest of the scientific community. They were well received as an analogue of ionic liquids (ILs) and a promising genre of "designer solvents." By definition, DESs are a class of eutectic mixtures resulting from mixing two or more components a hydrogen bond acceptor (HBA) and a hydrogen bond donor (HBD). DESs are typically characterized by a notable depression in the melting point of the resulting mixture, of which the interaction between the components yields deviations from the ideal behavior of a typical mixture.[2,3] An attractive feature of DESs is their simple synthesis procedure, cost efficiency, and biodegradability, depending on the choice of starting components. An example of such unique solvent systems is a category termed natural deep eutectic solvents (NADESs), in which natural components are used as HBAs and HBDs such as metabolites derived from biological organisms (*e.g.*, choline derivatives, alcohols, sugars, and organic and amino acids).[4] These versatile characteristics of DESs facilitated their use in different fields, such as extraction, catalysis, separation, and electrochemistry.[5,6]

Although DESs and ILs have similar features, including high thermal stability, negligible volatility, and a wide solvating capacity,[7] unlike their IL predecessors, DESs are not necessarily made exclusively of anions and cations. Different classes have been identified in the literature since the emergence of the term DESs.[8] Since DESs can also be formed from neutral species, they are not controlled by a charge balance ratio. Furthermore, compared to protonated ILs, the formation of a eutectic solvent does not require a full proton transfer.[9,10] Consequently, the molar ratio of their constituents can be modified according to the task, yielding a subsystem different from these constituents with variation in the physicochemical properties of the resulting DES.

The physical, physicochemical, and transport properties of DESs, such as boiling point, density, viscosity, surface tension, pH, vapor pressure, etc., are primarily determined by the interaction and structure of the DES's constituents. Such properties can be tailored by modifying the HBA and HBD structure and their corresponding molar ratios.[2,11] Like any solvent, the physicochemical properties of DESs play a pivotal

Received: January 21, 2023
Accepted: March 24, 2023
Published: March 30, 2023

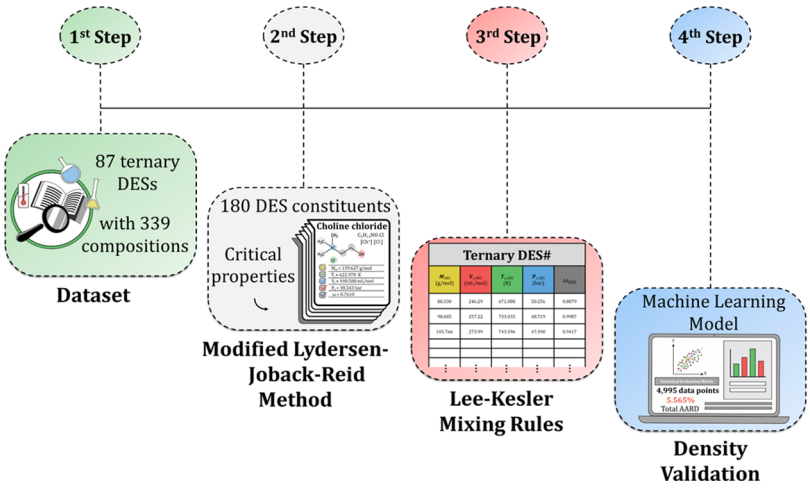

Figure 1. Visual representation of the methodology used in this study.

role in the feasibility and applicability of a specific chemical or physical process.[12−14] For example, the density of a solvent is of great importance in the separation between the aqueous and organic phases for hydrophobic DESs,[15,16] and the efficiency of solid−liquid extraction processes (*e.g.*, sugar extraction[17]). Likewise, the viscosity of a solvent affects the mass transfer from and to the solvent.[18,19] For a balanced process operation and design, careful choice of the DES and its constituent should be considered.[15] Such efforts considered combining more than two components of DESs or even diluting them with water (ternary DESs), adding another degree of freedom to the overall solvent design.[20] Being "designer solvents," ILs and DESs have virtually limitless combinations due to the wide range of cations, anions, and hydrogen bond donors that can be used to construct their molecular structure. As such, computational tools are essential for narrowing down the feasible combinations of DESs, as experimental investigations can be expensive and time-consuming. Thermodynamic models such as COSMO-RS can be useful tools for predicting the physicochemical properties of DESs and ILs.[12−14] These models can provide insights into the molecular-level interactions between the components and aid in the selection and design of appropriate solvent systems for specific applications. Additionally, the UNIFAC-Lei model has been widely employed in the prediction of the phase equilibrium of ILs.[21,22]

In addition to the physicochemical properties of DESs, critical properties (*i.e.*, critical temperature, pressure, and volume) are of paramount importance for many applications. For example, in order to develop thermodynamic models for the phase equilibria of these solvents, there is a need for numerical values of their critical properties. However, all DESs will thermally decompose at high temperatures; therefore, their critical properties are extremely difficult to determine experimentally and have to be predicted using appropriate models.[15,23] Several methods have been adopted in the literature to estimate the critical properties of solvents.[24,25] One of the most commonly used methods is the group contribution (GC) method, which, as the term implies, uses the properties and contributions of the constituent functional groups and their number of occurrences within a molecule to estimate the overall critical properties of that compound, whether it be a pure component or a mixture.[24,25] Although GC was not originally designed for ILs, it proved effective in estimating their critical properties.[24,26] Valderrama and co-workers[25−27] successfully evaluated the critical properties of thousands of ILs using the GC method using the modified Lydersen−Joback−Reid method (LJR). The method was tested by calculating the density and vapor pressure of different ILs.[26] Given its similarity to ILs, this framework was further extended to binary DESs *via* Lee−Kesler mixing rules by different research groups.[28,29] For example, Adeyemi et al.[29] estimated the critical properties of some choline chloride-based binary DESs. The method has also been used to estimate the critical properties of other types of binary DESs, including those prepared with solely neutral HBAs and HBDs (such as thymol and menthol).[15,30] Although the modified LJR method combined with Lee−Kesler's rules of mixing is adequate for estimating the critical properties of ILs and binary DESs, the technique was not used for DESs with more than two constituents. Ternary DESs are required for many applications in designing task-specific DESs. Therefore, an extension of this method is required in order to account for ternary mixtures. To the best of our knowledge, no previous alternative method for estimating the critical properties of ternary DESs has been reported in the literature.

Consequently, this paper presents a framework for computing the critical properties and acentric factors of ternary DESs by combining the modified LJR method with an extension of Lee−Kesler mixing rules. The reported framework was applied to a data set comprising 87 ternary DESs with 334 distinct compositions. To validate the method, the estimated critical properties and acentric factors of the DESs were used to predict their densities and compare them to the experimentally reported results. Figure 1 illustrates the methodology framework utilized in this investigation. The developed framework was also incorporated into an easy-to-use Excel spreadsheet to facilitate solvent selection and development of new processes using ternary DESs.

2. METHODOLOGY

2.1. Critical Properties of the DES Constituents. Many methods have been reported for calculating critical properties based on the group contribution in the literature. However, the most commonly used method for ILs and binary DESs is the modified Lydersen−Joback−Reid (LJR) group contribution method reported by Valderrama et al.[25] The authors defined several structural groups, and based on the frequency of the

https://doi.org/10.1021/acsomega.3c00436
ACS Omega 2023, 8, 13177−13191

Table 1. Functional Groups and Their Contributions to the Critical Properties as Defined in the Modified LJR Method[25,26]

#	group	ΔM_i	ΔT_{bMi}	ΔV_{cM}	ΔT_{cMi}	ΔP_{cMi}
			Without Rings			
1	$-CH_3$	15.035	23.58	66.81	0.0275	0.3031
2	$-CH_2-$	14.027	22.88	57.11	0.0159	0.2165
3	>CH−	13.019	21.74	45.70	0.0002	0.1140
4	>C<	12.011	18.18	21.78	−0.0206	0.0539
5	$=CH_2$	14.027	24.96	60.37	0.0170	0.2493
6	=CH−	13.019	18.25	49.92	0.0182	0.1866
7	=C<	12.011	24.14	34.90	−0.0003	0.0832
8	=C=	12.011	26.15	33.85	−0.0029	0.0934
9	°CH	13.019	21.74	43.97	0.0078	0.1429
10	°C−	12.011	18.18	43.97	0.0078	0.1429
11	−OH (alcohol)	17.008	92.88	30.40	0.0723	0.1343
12	−O−	16.000	22.42	15.61	0.0051	0.1300
13	>C=O	28.011	94.97	69.76	0.0247	0.2341
14	−CHO	29.019	72.24	77.46	0.0294	0.3128
15	−COOH	45.018	169.06	88.60	0.0853	0.4537
16	−COO-	44.010	81.10	84.76	0.0377	0.4139
17	HCOO−	45.018	169.06	97.77	0.0360	0.4752
18	=O (others)	16.000	−10.50	44.03	0.0273	0.2042
19	$-NH_2$	16.023	73.23	49.10	0.0364	0.1692
20	>NH	15.015	50.17	78.96	0.0119	0.0322
21	>N−	14.007	11.74	26.70	−0.0028	0.0304
22	−N=	14.007	74.60	45.54	0.0172	0.1541
23	−CN	26.018	125.66	89.32	0.0506	0.3697
24	$-NO_2$	46.006	152.54	123.62	0.0448	0.4529
25	−F	18.999	−0.03	31.47	0.0228	0.2912
26	−Cl	35.453	38.13	62.08	0.0188	0.3738
27	−Br	79.904	66.86	76.60	0.0124	0.5799
28	−I	126.905	93.84	100.79	0.0148	0.9174
29	−B	10.811	−24.56	22.45	0.0352	0.0348
30	−P	30.974	34.86	67.01	−0.0084	0.1776
31	−S−	32.066	117.52	184.67	0.0006	0.6901
32	$-NH_3$	17.031	73.23	49.10	0.0364	0.1692
33	$-SO_2$	64.065	147.24	112.19	−0.0563	−0.0606
34	−Al	26.982	22.55	96.92	−0.0316	−0.363
35	−Cu	63.546	−49.02	126.20	−0.1518	−0.3342
36	−Zn	65.409	227.14	150.35	−0.0877	−1.0705
			With Rings			
37	$-CH_2-$	14.027	27.15	51.64	0.0116	0.1982
38	>CH−	13.019	21.78	30.56	0.0081	0.1773
39	=CH−	13.019	26.73	42.55	0.0114	0.1693
40	>C<	12.011	21.32	17.62	−0.0180	0.0139
41	=C<	12.011	31.01	31.28	0.0051	0.0955
42	−O−	16.000	31.22	17.41	0.0138	0.1371
43	−OH (phenol)	17.008	76.34	−17.44	0.0291	0.0493
44	>C=O	28.011	94.97	59.32	0.0343	0.2751
45	>NH	15.015	52.82	27.61	0.0244	0.0724
46	>N−	14.007	52.82	25.17	0.0063	0.0538
47	−N=	14.007	57.55	42.15	−0.0011	0.0559

groups, the molecular weight (M), boiling temperature (T_b), critical volume (V_c), critical temperature (T_c), critical pressure (P_c), and acentric factor (ω) can be estimated as follows:

$$M(\text{g/mol}) = \sum z_i \Delta M_i \quad (1)$$

$$T_b(\text{K}) = 198.2 + \sum z_i \Delta T_{bMi} \quad (2)$$

$$V_c(\text{mL/mol}) = 6.75 + \sum z_i \Delta V_{cMi} \quad (3)$$

$$T_c(\text{K}) = \frac{T_b}{0.5703 + 1.0121 \sum z_i \Delta T_{cMi} - \left(\sum z_i \Delta T_{cMi}\right)^2} \quad (4)$$

$$P_c(\text{bar}) = \frac{M}{\left(0.2573 + \sum z_i \Delta P_{cMi}\right)^2} \quad (5)$$

https://doi.org/10.1021/acsomega.3c00436
ACS Omega 2023, 8, 13177−13191

Table 2. Calculated Properties for the 180 DES Constituents Considered in this Work

#	constitutent	M (g/mol)	V_c (mL/mol)	T_c (K)	P_c (bar)	ω	T_b (K)
1	1,2,4-triazole	69.067	203.76	683.556	113.493	0.3766	419.58
2	1,2-butanediol	90.124	294.28	646.126	47.600	0.9995	475.04
3	1,2-decanediol	174.286	636.94	781.296	24.357	1.1641	612.32
4	1,2-propanediol	76.097	237.17	623.361	56.601	0.9851	452.16
5	1,3-butanediol	90.124	294.28	646.126	47.600	0.9995	475.04
6	1,3-propanediol	76.097	238.88	621.748	55.080	0.9983	452.60
7	1,4-butanediol	90.124	295.99	644.568	46.518	1.0136	475.48
8	1,5-pentanediol	104.151	353.10	667.246	40.260	1.0353	498.36
9	1,6-hexanediol	118.178	410.21	689.832	35.486	1.0610	521.24
10	10-undecylenic acid	184.280	661.77	766.879	21.870	0.8867	587.50
11	1-butyl-1-methylpyrrolidinium bromide	222.170	620.03	761.658	25.712	0.4900	542.28
12	1-butyl-3-methyl imidazolium bromide	219.126	583.27	813.063	29.826	0.4891	571.42
13	1-butyl-3-methyl imidazolium chloride	174.675	568.75	767.315	27.850	0.4914	542.69
14	1-butylimidazolium chloride	160.648	504.38	740.865	32.599	0.5125	519.11
15	1-dodecanol	186.340	732.17	732.781	19.691	0.8953	566.34
16	1-ethyl-3-methyl imidazolium chloride	146.621	454.53	726.192	34.172	0.4164	496.93
17	1-hydroxyethyl-1,4-dimethyl-piperazinium bromide	239.158	618.49	886.258	28.221	0.8715	665.10
18	1-napthol	144.174	381.00	815.014	45.596	0.5061	554.68
19	1-tetradecanol	214.394	846.39	778.192	17.410	0.9691	612.10
20	2,2,2-trifluoroacetamide	113.042	241.80	575.017	44.821	0.4154	384.49
21	2,2,4-trimethyl-1,3-pentanediol	146.232	505.08	739.600	29.230	1.0067	562.82
22	2,3-butanediol	90.124	292.57	647.724	48.719	0.9854	474.60
23	2,6-dimethylphenol	122.168	344.42	719.708	41.917	0.5229	494.92
24	2-ethylhexyl 4-hydroxybenzoate	250.340	771.70	925.926	21.766	0.8645	707.88
25	2-furoic acid	112.086	271.69	737.363	53.201	0.6484	509.68
26	2-methoxybenzoic acid	152.151	410.53	813.208	37.574	0.6980	582.20
27	2-methyl-2,4-pentanediol	118.178	392.57	693.660	35.693	0.9592	517.50
28	3-amino-1-propanol	75.112	257.58	614.871	51.277	0.7393	432.95
29	4-amino-1,2,4-triazole	84.082	250.42	781.793	97.070	0.4344	492.81
30	4-chlorophenol	128.559	284.15	724.769	53.607	0.4558	481.61
31	4-ethylphenol	122.168	345.99	716.610	42.553	0.5003	489.94
32	acetamide	59.069	192.42	598.017	63.603	0.4322	389.98
33	acetic acid	60.053	162.16	581.831	58.395	0.5365	390.84
34	acetyl choline chloride	181.664	561.75	642.856	24.540	0.6104	469.25
35	alanine	89.095	256.96	694.821	52.939	0.7112	485.81
36	allyltriphenylphosphonium bromide	383.269	1049.85	1137.031	18.984	0.7003	859.99
37	aluminum chloride	133.341	289.91	563.464	129.251	0.2960	335.14
38	ammonium chloride	52.484	117.93	496.790	81.945	0.3283	309.56
39	anise alcohol	138.168	409.44	736.784	37.898	0.7189	528.90
40	arginine	174.205	603.40	971.561	45.324	1.1307	728.58
41	aspartic acid	133.105	335.86	876.521	48.048	1.1231	654.17
42	atropine	289.377	858.97	1065.224	20.473	1.0063	831.80
43	benzilic acid	228.249	635.59	1053.762	29.466	1.0694	807.64
44	benzimidazole	118.139	351.82	771.357	58.334	0.4153	504.24
45	benzoic acid	122.124	339.38	762.329	44.695	0.6266	531.92
46	benzotriazole	119.127	351.42	831.924	69.449	0.4082	535.06
47	benzyltriethylammonium chloride	227.779	768.43	769.787	19.952	0.6462	574.99
48	benzyltrimethylammonium chloride	185.698	597.10	705.436	24.929	0.5198	506.35
49	benzyltriphenylphosphonium chloride	388.878	1169.07	1232.701	16.926	0.7921	952.71
50	benzyltripropylammonium chloride	269.860	939.76	834.193	16.630	0.7720	643.63
51	betaine	117.149	375.75	559.551	35.081	0.4477	384.66
52	butanol	74.124	275.29	549.275	41.023	0.5902	383.30
53	butyl 4-hydroxybenzoate	194.232	544.97	843.350	30.075	0.7239	616.80
54	butylammonium bromide	154.051	370.59	632.708	40.142	0.4535	430.51
55	butyltriphenylphosphonium bromide	399.312	1120.59	1153.018	17.379	0.7651	886.12
56	camphor	152.238	487.22	749.461	30.303	0.3417	509.78
57	capric acid	172.269	619.04	759.498	22.844	0.8044	573.88
58	carnitine	161.203	508.96	700.386	30.681	0.8707	522.16
59	chloro benzoic acid	156.569	390.19	812.846	41.049	0.6602	574.33
60	choline chloride	139.627	440.58	622.970	30.543	0.7610	457.45
61	citric acid	192.127	438.95	1079.620	38.304	1.7011	862.20

https://doi.org/10.1021/acsomega.3c00436
ACS Omega 2023, 8, 13177−13191

Table 2. continued

#	constitutent	M (g/mol)	V_c (mL/mol)	T_c (K)	P_c (bar)	ω	T_b (K)
62	copper chloride	98.999	195.03	448.108	1123.079	−0.1633	187.31
63	coumarin	146.147	401.34	801.181	41.513	0.4822	546.79
64	decanol	158.286	617.95	687.562	22.656	0.8164	520.58
65	decyltrimethylammonium bromide	280.294	891.28	752.170	17.271	0.7527	577.04
66	dichloroacetic acid	128.943	265.21	684.472	52.139	0.5522	465.26
67	diethanolamine	105.139	374.95	705.931	51.842	1.1477	525.65
68	diethylamine hydrochloride	109.600	365.77	580.064	32.390	0.4600	402.48
69	diethylene glycol	106.124	311.60	672.216	45.819	1.0375	497.90
70	diethylenetriamine	103.169	412.35	696.376	46.228	0.6463	486.35
71	diethylethanolammonium chloride	153.654	484.76	720.727	28.284	0.8229	537.12
72	dimethyldodecyl-*n*-amine oxide	229.409	877.70	724.541	16.681	0.7173	554.78
73	dimethyloctadecyl-*n*-amine oxide	313.571	1220.36	861.199	12.505	0.9328	692.06
74	dodecylmorpholine-*n*-oxide	271.447	966.52	891.243	16.503	0.7762	688.52
75	dodecyltrimethylammonium bromide	308.348	1005.50	796.793	15.491	0.8327	622.80
76	ethanolamine hydrochloride	97.546	262.55	634.708	52.154	0.7644	448.20
77	ethylammonium bromide	125.997	256.37	587.302	54.107	0.3951	384.75
78	ethylammonium chloride	81.546	241.85	539.121	46.808	0.3764	356.02
79	ethylene glycol	62.070	181.77	598.731	67.505	0.9927	429.72
80	ethylenediamine	60.100	219.17	586.900	56.793	0.4800	390.42
81	formamide	45.042	133.31	543.295	82.409	0.3903	343.67
82	formic acid	45.018	95.35	565.576	89.053	0.5282	367.26
83	fructose	180.162	394.21	1016.552	43.875	2.1598	830.51
84	furfuryl alcohol	98.103	270.60	658.230	53.941	0.6710	456.38
85	glucose	180.162	386.07	1005.776	38.299	2.1275	825.60
86	glutamic acid	147.132	392.97	896.671	41.589	1.1429	677.05
87	glutamine	146.148	423.23	911.848	43.617	1.0174	676.19
88	glutaric acid	132.117	355.28	813.570	40.141	0.9954	604.96
89	glycerol	92.097	257.87	715.991	63.196	1.4577	544.34
90	glycine	75.068	201.56	670.937	62.414	0.7098	463.37
91	glycolic acid	76.053	182.86	674.800	67.458	0.9724	483.02
92	guaiacol	124.141	304.49	724.709	48.017	0.4893	489.48
93	hexafluoroisopropanol	168.043	315.23	490.047	30.156	0.5666	349.00
94	hexanol	102.178	389.51	596.230	32.351	0.6597	429.06
95	histidine	155.158	433.40	936.743	49.352	0.9199	679.95
96	hydrocinnamic acid	150.178	453.60	802.829	34.513	0.6887	577.68
97	ibuprofen	206.286	677.05	891.138	23.980	0.8301	673.30
98	imidazole	68.079	204.16	621.827	85.275	0.3581	388.76
99	isobutyl 4-hydroxybenzoate	194.232	543.26	845.691	30.455	0.7076	616.36
100	lactic acid	90.080	238.26	698.626	56.524	0.9648	505.46
101	lauric acid	200.323	733.26	803.149	19.821	0.8832	619.64
102	levulinic acid	116.118	346.14	745.555	41.083	0.7147	531.57
103	lidocaine	234.344	842.23	914.202	22.739	0.8049	691.26
104	malic acid	134.090	317.16	880.404	50.500	1.3882	673.82
105	malonic acid	104.063	241.06	772.083	54.549	0.9544	559.20
106	maltose	342.308	720.20	1655.686	22.030	1.0272	1289.66
107	mandelic acid	152.151	415.48	868.416	42.089	1.0304	646.54
108	mannose	180.162	386.07	1005.776	38.299	2.1275	825.60
109	melamine	126.123	374.34	1007.803	84.862	0.7339	683.57
110	menthol	156.270	529.88	715.575	24.195	0.6998	530.35
111	methionine	149.215	555.85	899.953	25.471	0.5562	649.09
112	methyl 4-hydroxybenzoate	152.151	373.64	783.437	42.513	0.6203	548.16
113	methyldiethanolamine	119.166	389.50	679.458	40.029	1.0866	510.80
114	methylmorpholine-*n*-oxide	117.150	338.31	661.099	41.800	0.3404	436.84
115	methylphenol	108.141	288.88	695.624	49.511	0.4731	467.06
116	methyltrioctylammonium bromide	448.618	1576.60	1033.966	10.217	1.0275	851.60
117	methyltrioctylammonium chloride	404.167	1562.08	998.318	9.805	1.0009	822.87
118	methyltriphenylphosphonium bromide	357.231	949.26	1099.800	20.803	0.6343	817.48
119	monochloroacetic acid	94.498	214.54	632.271	55.804	0.5607	428.27
120	monoethanolamine	61.085	200.47	591.937	61.850	0.7234	410.07
121	myristic acid	228.377	847.48	847.211	17.504	0.9574	665.40
122	*n*,*n*-dimethyl urea	88.111	285.93	632.761	52.362	0.4986	425.30

https://doi.org/10.1021/acsomega.3c00436
ACS Omega 2023, 8, 13177−13191

Table 2. continued

#	constitutent	M (g/mol)	V_c (mL/mol)	T_c (K)	P_c (bar)	ω	T_b (K)
123	ninhydrin	178.147	436.57	1003.709	46.458	1.2832	764.16
124	nitrobenzoic acid	167.122	451.73	951.442	40.471	0.8035	688.74
125	nonanoic acid	158.242	561.93	737.725	24.730	0.7647	551.00
126	octanoic acid	144.215	504.82	715.928	26.954	0.7255	528.12
127	octanol	130.232	503.73	642.177	26.660	0.7365	474.82
128	octyl 4-hydroxybenzoate	250.340	773.41	924.057	21.563	0.8802	708.32
129	oleic acid	282.469	1061.54	924.906	14.470	1.1075	747.66
130	oxalic acid	90.036	183.95	751.296	66.372	0.9453	536.32
131	palmitic acid	256.431	961.70	891.999	15.672	1.0227	711.16
132	phenol	94.114	233.34	671.266	60.368	0.4296	439.20
133	phenylacetic acid	136.151	396.49	782.611	38.956	0.6559	554.80
134	phosphocholine chloride	219.609	597.63	762.130	28.330	1.2642	597.11
135	proline	115.133	308.44	746.030	47.596	0.6838	523.31
136	propionic acid	74.080	219.27	604.859	48.918	0.5578	413.72
137	propylammonium bromide	140.024	313.48	610.204	46.117	0.4223	407.63
138	pyruvic acid	88.064	231.92	703.504	56.524	0.6682	485.81
139	resorcinol	110.114	204.63	772.756	73.487	0.6329	519.82
140	serine	105.095	277.66	782.336	58.095	1.1411	577.99
141	sorbitol	182.178	486.17	1076.848	47.807	2.4083	888.20
142	stearic acid	284.485	1075.92	937.818	14.186	1.0745	756.92
143	succinimide	99.091	256.28	734.367	60.832	0.5732	495.26
144	sucrose	342.308	733.81	1640.421	23.486	1.1653	1290.30
145	tartaric acid	150.090	336.15	968.922	54.382	1.8122	765.56
146	tetrabutylammonium bromide	322.375	1062.61	819.279	14.731	0.8699	645.68
147	tetrabutylammonium chloride	277.924	1048.09	780.385	13.898	0.8578	616.95
148	tetrabutylammonium hydrogen sulfate	339.544	1144.21	1063.080	18.348	1.0602	841.36
149	tetrabutylphosphonium bromide	339.342	1102.92	851.015	14.575	0.8369	668.80
150	tetrabutylphosphonium chloride	294.891	1088.40	811.839	13.821	0.8290	640.07
151	tetradecyltrimethylammonium bromide	336.402	1119.72	841.934	14.042	0.9045	668.56
152	tetraethylammonium bromide	210.159	605.73	640.639	24.215	0.5404	462.64
153	tetraethylammonium chloride	165.708	591.21	597.470	22.074	0.5277	433.91
154	tetraethylammonium *p*-toluene sulfonate	301.453	956.50	1031.959	23.173	0.6163	757.96
155	tetraethylene glycol	194.232	571.26	814.776	27.702	1.1814	634.26
156	tetraethylenepentamine	189.307	798.71	900.322	32.210	0.9761	678.21
157	tetraheptylammonium chloride	446.248	1733.41	1078.808	8.928	0.9456	891.51
158	tetrahexylammonium bromide	434.591	1519.49	1008.542	10.577	1.0313	828.72
159	tetramethylammonium chloride	109.600	362.77	502.076	31.212	0.3629	342.39
160	tetraoctylammonium bromide	546.807	1976.37	1229.453	8.248	0.8281	1011.76
161	tetraoctylammonium chloride	502.356	1961.85	1195.694	7.977	0.7895	983.03
162	tetrapropylammonium bromide	266.267	834.17	729.949	18.324	0.7108	554.16
163	tetrapropylammonium chloride	221.816	819.65	689.131	17.059	0.7003	525.43
164	tetrazole	70.055	203.36	748.003	157.608	0.4010	450.40
165	threonine	119.122	333.06	805.249	49.865	1.1366	600.43
166	thymol	150.222	456.93	763.553	33.289	0.5739	540.24
167	toluenesulfonic acid	172.206	448.91	954.457	76.302	0.5616	630.84
168	toluic acid	136.151	394.92	785.641	38.428	0.6796	559.78
169	trichloroacetic acid	163.388	303.37	736.995	45.920	0.4916	499.83
170	triethanolamine	149.193	467.31	794.486	37.689	1.5214	625.86
171	triethylene glycol	150.178	441.43	743.934	34.549	1.1058	566.08
172	triethylenetetramine	146.238	605.53	800.100	38.102	0.8104	582.28
173	triethylsulfonium bis(trifluoromethylsulfonyl)imide	357.324	875.31	1156.262	27.254	0.0384	728.86
174	trioctylphosphine oxide	386.646	1517.53	942.048	10.408	1.0143	773.78
175	urea	60.057	174.71	666.638	87.220	0.5959	439.63
176	xylitol	152.151	410.07	950.567	52.413	2.2412	773.58
177	xylose	150.135	319.64	892.796	44.393	1.8599	715.21
178	zinc bromide	225.217	310.30	1112.153	1874.753	0.3829	559.06
179	zinc chloride	136.315	281.26	970.056	31676.411	1.0134	501.60
180	water	18.015	55.90	647.100	220.550	0.3450	373.20

https://doi.org/10.1021/acsomega.3c00436
ACS Omega 2023, 8, 13177−13191

Table 3. Calculated Properties for the Ternary DESs Considered in this Work

#	deep eutectic solvent	M_{DES} (g/mol)	$V_{c,DES}$ (mL/mol)	$T_{c,DES}$ (K)	$P_{c,DES}$ (bar)	ω_{DES}
1	1-butylimidazolium chloride: copper chloride: zinc chloride (1:1:0.8)	131.678	321.26	685.481	45.289	0.4143
2	alanine: citric acid: water (1:1:3)[35]	67.053	151.53	721.091	91.752	0.6895
3	alanine: malic acid: water (1:1:3)[35]	55.446	133.80	686.341	101.173	0.6269
4	allyltriphenylphosphonium bromide: diethylene glycol: water (1:4:2.36)[36]	115.506	288.63	703.834	45.637	0.7696
5	benzyltriethylammonium chloride: toluenesulfonic acid: water (0.43:1:1)[37]	118.523	299.80	767.019	52.983	0.4873
6	benzyltrimethylammonium chloride: oxalic acid: water (1:1:2)[38]	77.941	190.92	657.990	70.122	0.5388
7	benzyltrimethylammonium chloride: toluenesulfonic acid: water (0.43:1:1)[38]	111.097	277.17	758.109	57.076	0.4650
8	betaine: oxalic acid: water (1:2:4)[39]	52.741	125.39	644.009	104.773	0.5312
9	choline chloride: citric acid: water (1:1:1)[35,40]	116.590	284.58	756.037	46.600	0.9357
10	choline chloride: ethylene glycol: water (1:2:0.75)[41]	73.885	210.94	601.971	52.774	0.8009
11	choline chloride: fructose: water (2:1:0.8)[35,40,42,43]	124.763	328.18	710.968	36.373	1.0420
12	choline chloride: glucose: water (6:3:1)[35,40,43−45]	139.626	375.18	724.273	31.220	1.1293
13	choline chloride: glycerol: water (1:2:0.75)[41]	89.883	251.83	664.763	44.195	1.0486
14	choline chloride: malic acid: water (1:1:2)[35]	77.437	192.65	673.301	66.885	0.7098
15	choline chloride: malonic acid: water (1:2:0.76)[46]	96.220	242.87	692.888	53.175	0.7803
16	choline chloride: maltose: water (1:0.4:1)[40]	122.736	286.39	759.141	52.185	0.6320
17	choline chloride: mannose: water (1:1:0.55)[43]	129.172	316.87	756.872	37.330	1.2062
18	choline chloride: sucrose: water (1:0.4:1)[40]	122.736	288.05	757.239	51.326	0.6550
19	choline chloride: toluenesulfonic acid: water (2:1:1)[40,47]	117.385	323.30	692.170	42.523	0.6073
20	choline chloride: triethylene glycol: water (3:6:1)[44]	133.796	391.54	691.047	31.076	0.9263
21	choline chloride: urea: water (1:2:0.75)[48]	72.867	207.20	636.806	61.422	0.5898
22	choline chloride: xylose: water (1:1:1)[40,43]	102.592	249.60	698.795	48.061	0.9886
23	fructose: citric acid: water (1:1:2)[35]	102.080	208.04	825.139	63.908	1.1377
24	fructose: malic acid: water (1:1:3)[35]	73.659	154.74	747.479	85.382	0.9166
25	fructose: urea: water (1:1:2)[35]	69.062	152.71	726.706	85.969	0.8614
26	glucose: citric acid: water (1:1:2)[35]	102.080	206.41	822.667	64.446	1.1296
27	glucose: malic acid: water (1:1:3)[35]	73.659	153.55	745.625	86.055	0.9101
28	glucose: urea: water (1:1:2)[35]	69.062	151.22	724.414	86.818	0.8534
29	tetrabutylammonium chloride: toluenesulfonic acid: water (1:1:1)[47]	156.048	447.54	759.553	33.938	0.5881
30	tetrabutylphosphonium chloride: toluenesulfonic acid: water (1:1:1)[47]	161.704	457.56	770.118	33.771	0.5785
31	choline chloride: ethylene glycol: urea (1:2:1)[49]	80.956	237.47	616.364	47.363	0.8356
32	zinc bromide: 1-butyl-3-methyl imidazolium bromide: urea (1:1:1)[50]	168.078	342.56	847.687	51.211	0.4894
33	zinc chloride: 1-butyl-3-methyl imidazolium chloride: urea (1:1:1)[50]	123.657	328.48	788.989	46.130	0.7001
34	tetrabutylammonium bromide: octanoic acid: thymol (1:3:1)[51]	181.048	595.12	743.042	23.768	0.7240
35	acetamide: urea: sorbitol (1:1.5:0.83)[52]	90.291	248.64	740.085	50.861	0.9999
36	4-amino-1,2,4-triazole: glycerol: resorcinol (1:5:4)[53]	98.502	235.36	744.234	53.461	1.0254
37	zinc bromide: 1-butyl-3-methyl imidazolium bromide: *n*,*n*-dimethyl urea (1:1:1)[50]	177.439	386.06	836.863	45.358	0.4569
38	zinc chloride: 1-butyl-3-methyl imidazolium chloride: *n*,*n*-dimethyl urea (1:1:1)[50]	133.018	371.36	779.066	40.772	0.6676
39	phosphocholine chloride: dichloroacetic acid: lauric acid (1:1:1)[54]	182.958	517.93	745.679	25.619	0.8998
40	ammonium chloride: melamine: lactic acid (1:1:7)[55]	89.907	237.33	707.077	53.677	0.8684
41	betaine: 1,2-propanediol: lactic acid (1:3:1)[56]	87.104	263.42	622.996	42.523	0.8736
42	betaine: 1,3-propanediol: lactic acid (1:3:1)[57]	87.104	264.48	622.067	42.158	0.8815
43	betaine: ethylene glycol: lactic acid (1:1:1)[56,57]	89.766	261.24	613.979	43.450	0.8018
44	choline chloride: acetamide: lactic acid (1:2:3)[56,57]	88.001	252.83	649.015	48.336	0.7533
45	choline chloride: ethylene glycol: lactic acid (1:2:1)[56,57]	88.462	254.28	625.227	43.266	0.9278
46	choline chloride: urea: lactic acid (1:2:3)[56,57]	88.330	246.29	671.088	50.256	0.8079
47	malic acid: alanine: lactic acid (1:1:3)[56,57]	98.685	257.22	733.035	48.719	0.9987
48	malic acid: proline: lactic acid (1:2:3)[56,57]	105.766	273.99	743.596	47.490	0.9417
49	zinc chloride: fructose: glycine (1:1:1)[58]	130.515	288.77	880.556	45.758	1.2943
50	zinc chloride: glucose: glycine (1:1:1)[58]	130.515	286.32	877.159	46.205	1.2836
51	1-butyl-1-methylpyrrolidinium bromide: choline chloride: glycerol (3:1:2)[59]	165.055	458.95	718.664	28.330	0.8577
52	betaine: ethylene glycol: glycerol (1:2:2)[56,57]	85.097	247.85	633.727	42.428	1.0697
53	betaine: urea: glycerol (1:2:3)[56,57]	85.592	246.87	669.130	46.270	1.0021
54	choline chloride: malic acid: glycerol (2:3:1)[60]	128.937	346.22	759.384	34.520	1.1907
55	choline chloride: oxalic acid: glycerol (1:1:3)[61]	101.191	275.71	699.461	39.477	1.2159
56	choline chloride: urea: glycerol (2:3:1)[62]	91.920	269.12	653.376	45.008	0.7946
57	ethylammonium chloride: zinc chloride: glycerol (2:6:1)[63]	119.231	269.73	836.376	54.708	0.9212
58	urea: acetamide: glycerol (1:2:3)[56]	75.748	221.20	667.409	52.146	0.9722
59	zinc chloride: fructose: glutamine (1:1:1)[58]	154.208	364.42	964.075	37.782	1.3969

https://doi.org/10.1021/acsomega.3c00436
ACS Omega 2023, 8, 13177−13191

Table 3. continued

#	deep eutectic solvent	M_{DES} (g/mol)	$V_{c,DES}$ (mL/mol)	$T_{c,DES}$ (K)	$P_{c,DES}$ (bar)	ω_{DES}
60	zinc chloride: glucose: glutamine (1:1:1)[58]	154.208	361.77	960.539	38.120	1.3861
61	1-ethyl-3-methyl imidazolium chloride: diethylenetriamine: ethylene glycol (2:1:1)[64]	114.620	368.64	684.230	36.726	0.6179
62	choline chloride: 1,2,4-triazole: ethylene glycol (0.43:1:2)[65]	73.805	216.62	623.177	53.544	0.7841
63	choline chloride: imidazole: ethylene glycol (0.43:1:2)[65]	73.517	216.74	605.839	52.132	0.7787
64	choline chloride: oxalic acid: ethylene glycol (1:1:1)[61]	97.218	260.41	649.050	44.352	0.8998
65	choline chloride: phenol: ethylene glycol (1:5:4)[66]	85.848	230.41	635.070	53.171	0.6880
66	choline chloride: tetrazole: ethylene glycol (0.43:1:2)[65]	74.094	216.50	640.699	54.931	0.7912
67	diethylenetriamine: acetamide: ethylene glycol (1:1:1)[67]	74.769	255.64	627.965	47.346	0.6904
68	diethylethanolammonium chloride: copper chloride: ethylene glycol (1:1:1)[68]	104.908	276.95	582.900	42.643	0.5508
69	methyltriphenylphosphonium bromide: glycerol: ethylene glycol (1:2:2)[69]	133.113	337.24	733.677	35.527	1.1070
70	zinc chloride: glycerol: ethylammonium chloride (1:6:2)[63]	94.659	256.83	700.585	43.370	1.1680
71	alanine: lactic acid: citric acid (1:3:1)[56,57]	110.292	279.03	769.532	45.927	1.0613
72	betaine: glycerol: citric acid (1:2:1)[56,57]	123.368	329.59	757.168	34.933	1.2660
73	proline: glycerol: citric acid (1:4:1)[56,57]	112.608	294.32	778.128	38.273	1.3693
74	proline: lactic acid: citric acid (1:3:1)[56,57]	115.500	289.33	779.913	44.994	1.0558
75	tetrabutylammonium bromide: lauric acid: capric acid (1:0.86:1.14)[70]	230.320	792.20	790.326	18.112	0.8487
76	tetrabutylammonium bromide: oleic acid: capric acid (1:1.2:0.8)[70]	266.334	935.99	843.635	15.735	0.9474
77	choline chloride: urea: arginine (1:2:0.2)[71]	92.040	273.11	663.209	46.971	0.6807
78	urea: glycerol: acetamide (1:2:3)[57]	70.243	210.43	647.747	56.918	0.8013
79	zinc bromide: 1-butyl-3-methyl imidazolium bromide: acetamide (1:1:1)[50]	167.749	349.90	823.724	49.629	0.4347
80	zinc chloride: 1-butyl-3-methyl imidazolium chloride: acetamide (1:1:1)[50]	123.327	335.71	765.873	44.696	0.6455
81	thymol: menthol: 2,2,4-trimethyl-1,3-pentanediol (1:1:1)[15]	150.908	496.99	739.168	27.934	0.7601
82	thymol: capric acid: 2,2,4-trimethyl-1,3-pentanediol (1:1:1)[15]	156.241	525.59	753.615	26.576	0.7950
83	thymol: trioctylphosphine oxide: 2,2,4-trimethyl-1,3-pentanediol (1:1:1)[15]	227.700	783.28	806.456	18.574	0.8650
84	thymol: lidocaine: 2,2,4-trimethyl-1,3-pentanediol (1:1:1)[15]	176.933	593.81	803.637	25.083	0.7952
85	choline chloride: malonic acid: 1,3-propanediol (1:1:3)[57]	94.396	276.41	648.274	41.034	0.9421
86	choline chloride: malonic acid: 1,2-propanediol (1:1:3)[56]	94.396	275.33	649.219	41.386	0.9342
87	choline chloride: oxalic acid: 1,2-propanediol (1:1:3)[61]	91.591	262.96	644.066	43.020	0.9323

$$\omega = \frac{(T_b - 43)(T_c - 43)}{(T_c - T_b)(0.7T_c - 43)}\log\left(\frac{P_c}{1.01325}\right) - \frac{(T_c - 43)}{(T_c - T_b)}\log\left(\frac{P_c}{1.01325}\right) + \log\left(\frac{P_c}{1.01325}\right) - 1 \quad (6)$$

where z_i represents the number of occurrences of group i in the molecular structure, ΔM_i is the molecular mass of group i, ΔT_{bMi} is the boiling temperature contribution of group i, ΔV_{cMi} is the critical volume contribution of group i, ΔT_{cMi} is the critical temperature contribution of group i, and ΔP_{cMi} is the critical pressure contribution of group i. The group contribution values of each functional group in the modified LJR method are summarized in Table 1. Using eqs 1−6, the determined properties of the 180 DES constituents considered in this work are presented in Table 2. For a detailed description of the modified LJR method, the reader is referred to the work of Valderrama et al.[25,26]

2.2. Extended Lee−Kesler Mixing Rules. The Lee−Kesler mixing rules can be used to calculate the critical properties of a binary mixture using the critical properties of its constituents, as reported in the literature for binary DESs.[30,31] In the present work, the definitions of the Lee−Kesler mixing rules have been extended to ternary mixtures to determine the critical properties and acentric factors of 87 ternary DESs using eqs 7−15, as suggested by Plocker et al.[32] As can be observed, if x_3 is set to 0, then the binary version that has been applied to binary DESs previously in the literature is obtained.[28,29]

$$M_{DES}(\text{g/mol}) = \sum_{n=1}^{3} x_n M_n \quad (7)$$

$$M_{DES} = x_1M_1 + x_2M_2 + x_3M_3 \quad (8)$$

$$V_{c,DES}(\text{mL/mol}) = \sum_{n=1}^{3}\sum_{m=1}^{3} x_n x_m V_{c,nm} \quad (9)$$

$$V_{c,DES} = x_1x_1V_{c,11} + x_2x_2V_{c,22} + x_3x_3V_{c,33} + 2x_1x_2V_{c,12} + 2x_1x_3V_{c,13} + 2x_2x_3V_{c,23} \quad (10)$$

$$T_{c,DES}(\text{K}) = \frac{1}{V_{c,DES}^{0.25}}\sum_{n=1}^{3}\sum_{m=1}^{3} x_n x_m V_{c,nm}^{0.25} T_{c,nm} \quad (11)$$

$$T_{c,DES} = \frac{1}{V_{c,DES}^{0.25}}(x_1x_1V_{c,11}^{0.25}T_{c,11} + x_2x_2V_{c,22}^{0.25}T_{c,22} + x_3x_3V_{c,33}^{0.25}T_{c,33} + 2x_1x_2V_{c,12}^{0.25}T_{c,12} + 2x_1x_3V_{c,13}^{0.25}T_{c,13} + 2x_2x_3V_{c,23}^{0.25}T_{c,23}) \quad (12)$$

$$P_{c,DES}(\text{bar}) = (0.2905 - 0.0850\omega_{DES})\frac{83.1447T_{c,DES}}{V_{c,DES}} \quad (13)$$

$$\omega_{DES} = \sum_{n=1}^{3} x_n\omega_n \quad (14)$$

$$\omega_{DES} = x_1\omega_1 + x_2\omega_2 + x_3\omega_3 \quad (15)$$

https://doi.org/10.1021/acsomega.3c00436
ACS Omega 2023, 8, 13177−13191

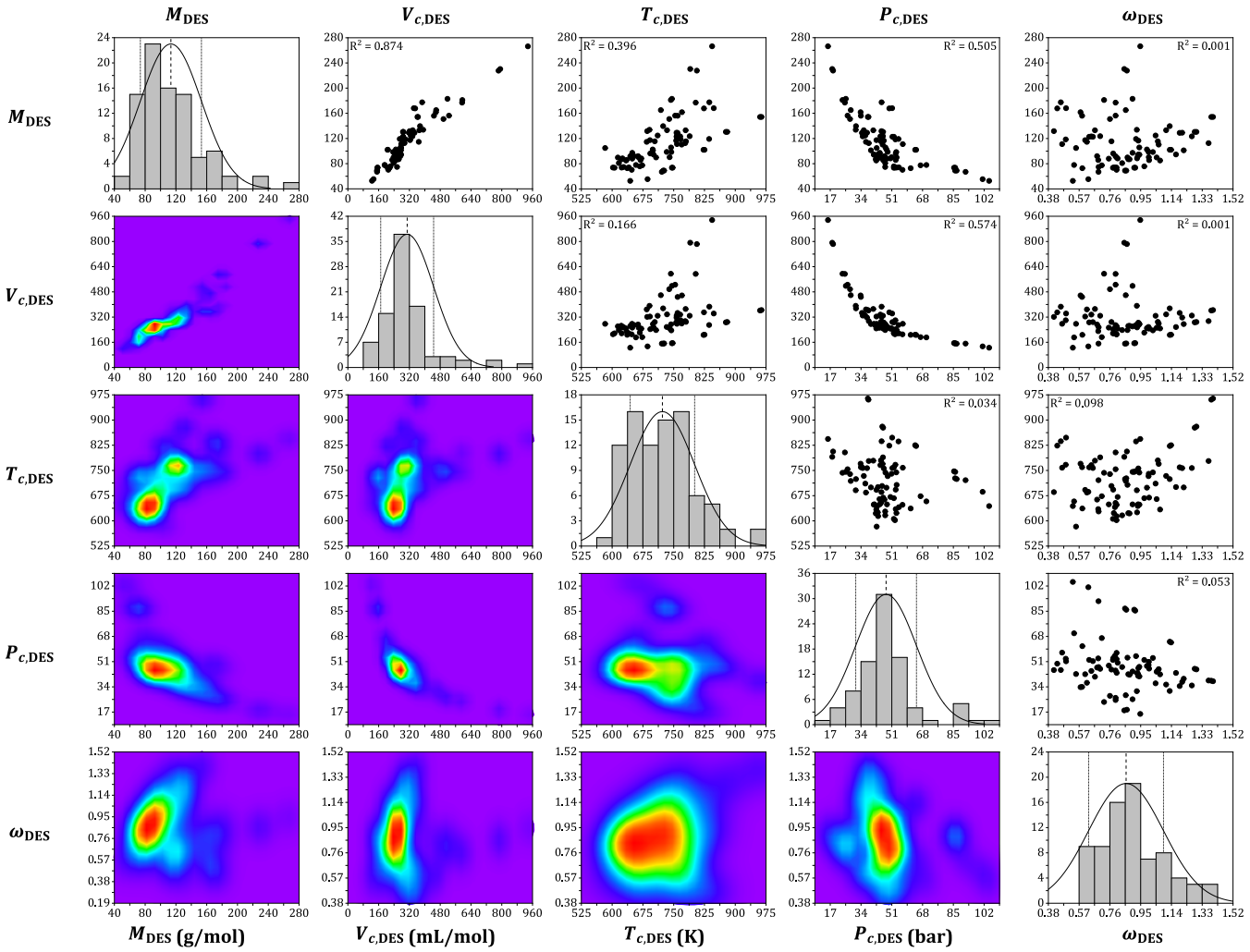

Figure 2. Scatter matrix representation of the calculated properties for the 87 ternary DESs in this work. The purple regions in the contour plots denote regions of low data density, while the red regions denote high density.

where the binary interaction terms $V_{c,nm}$ and $T_{c,nm}$ are expressed as follows:[32]

$$V_{c,nm}(\text{mL/mol}) = \frac{1}{8}(V_{c,n}{}^{1/3} + V_{c,m}{}^{1/3})^3 \quad (16)$$

$$T_{c,nm}(\text{K}) = (T_{c,n}T_{c,m})^{0.5} \quad (17)$$

The complete method utilized to determine the calculated properties has been imported into an open-source and easy-to-use Excel program available in the Supporting Information (SI) accompanying this manuscript in Table S1.

3. RESULTS AND DISCUSSION

The data set used in this work consisted of 87 ternary DESs obtained from 43 references, including 67 unique components with 334 distinct compositions. Table 3 summarizes all 87 ternary DESs and their corresponding references. It can be observed from the data set that the ternary DESs considered in this work cover a broad range of structural variety with different functional groups and different compositions, leading to some DESs being hydrophilic and others being hydrophobic. The calculated properties (M_{DES}, $V_{c,DES}$, $T_{c,DES}$, $P_{c,DES}$, and ω_{DES}) for the 87 ternary DESs are also presented in Table 3, which were determined based on a specific representative molar ratio. The properties are also graphically depicted in Figure 2 as density contour plots (lower triangular matrix), distribution histograms (diagonal), and $x-y$ scatter plots (upper triangular matrix). The degree of multicollinearity between the input variables was also determined using the variance inflation factor (VIF), which ranged between 1.0 and 7.9, indicating negligible multicollinearity of the properties (VIF < 10.0).[33,34] It should be noted that the full list for all 334 ternary compositions is also available in the SI in Table S2. Furthermore, in addition to the characterization of the critical properties and acentric factors of ternary DESs, Table S2 includes the critical properties and acentric factors of 260 unique binary DES mixtures with 573 compositions based on the 163 constituents from Table 2. The critical property characterizations of DESs reported in this study can serve as a valuable database for designing new molecular-based models that aid in predicting the properties of DESs, which can help drive their application in a wide range of industries and fields.

To showcase the calculated properties across the chemical space, ternary plots of all five properties have been determined throughout the compositional range for DES#45, choline chloride:ethylene glycol:lactic acid (ChCl:LA:EG), as shown in Figure 3A–E. The numerical values are also reported in Table S3. First, it can be observed that the values M_{DES} and

https://doi.org/10.1021/acsomega.3c00436
ACS Omega 2023, 8, 13177−13191

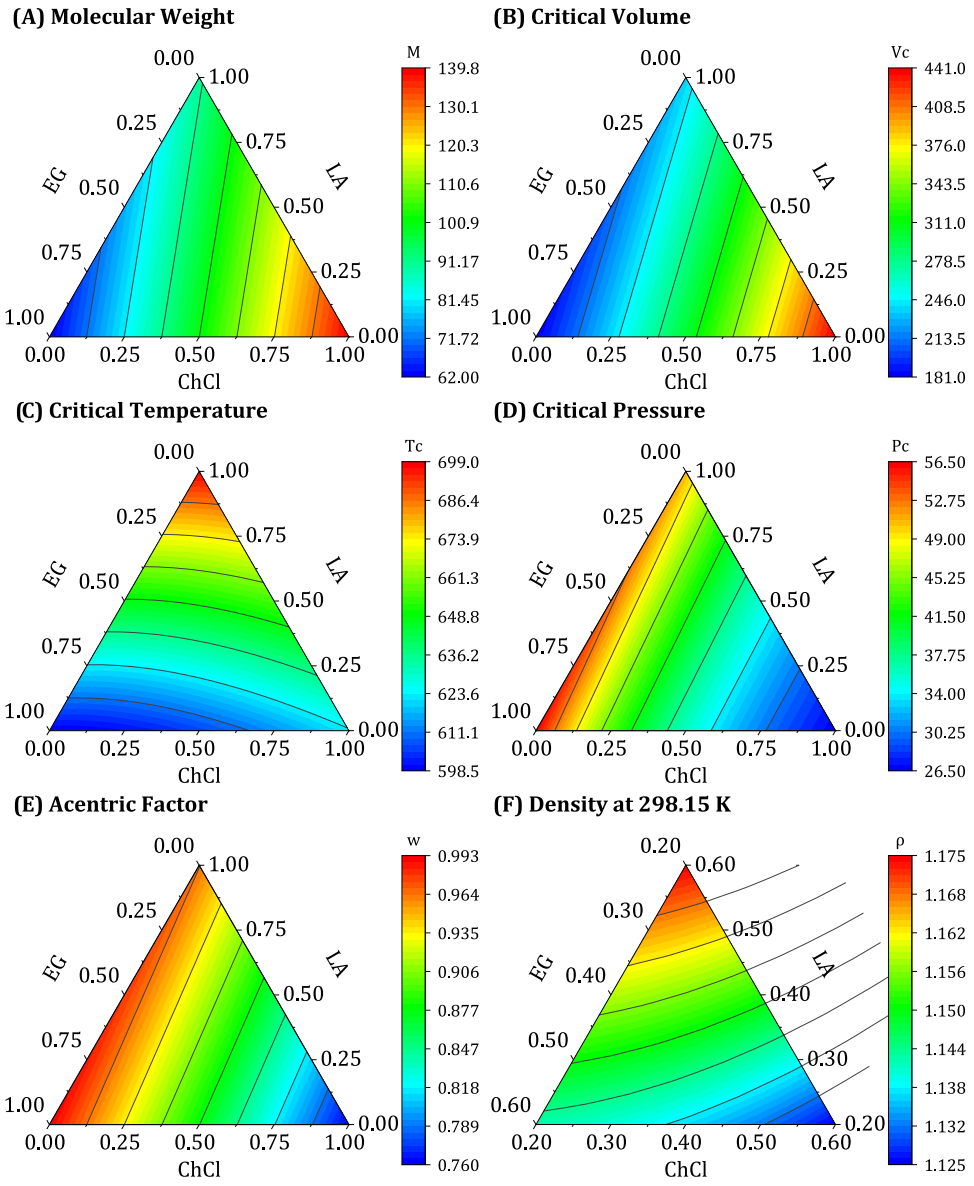

Figure 3. Ternary plots showing the calculated properties of ChCl:LA:EG across the entire compositional range for A) molecular weight, B) critical volume, C) critical temperature, D) critical pressure, E) acentric factor, and F) density at 298.15 K.

$V_{c,DES}$ are maximized with increasing ChCl content, whereas increasing the EG content tends to increase $P_{c,DES}$ and ω_{DES}. It can also be observed from the figure that the method is reliable as the values calculated are within reasonable boundaries between the values of the pure constituents (Table 2). Thus, it can be concluded that the modified LJR method coupled with Lee−Kesler mixing rules can be utilized to describe a ternary DES mixture reasonably. The importance of the framework developed in this work is that it can be used (i) to extend pre-existing models available in the literature for binary DESs to ternary DESs and (ii) to facilitate the development of computational models for ternary DESs using the calculated critical properties and acentric factors as inputs, which have not been reported in the literature yet.

To validate the method, the estimated critical properties and acentric factors of the DESs were used to predict their densities and compare them to the experimental values reported in the literature. Regarding the models developed for binary DESs, Haghbakhsh et al.[72] developed a generalized model for predicting the density of DESs that considers 1239 data points of 149 DES compositions. Their model achieved an average absolute relative deviation (AARD) of 3.12% in predicting their data set, which is expressed as follows:[72]

$$\rho(\mathrm{g/mL}) = -1.13 \times 10^{-6}(T_{c,DES}{}^{2}) + 2.566 \times 10^{-3}(T_{c,DES}) + 0.2376(\omega_{DES}{}^{0.2211}) - 4.67 \times 10^{-4}(V_{c,DES}) - 4.64 \times 10^{-4}(T) \quad (18)$$

The advantage of utilizing the Haghbakhsh model is that no experimental reference density is required as input.[72] Different models can also be used to validate the reliability of the estimated critical properties and acentric factors. Nevertheless, they require a single reference density measurement in addition to the critical properties of the DESs, such as the modified Rackett equation,[23] thereby achieving higher accuracies. The predicted densities of all 87 ternary DESs considered in this work using the Haghbakhsh model are presented in Table S4 in full detail with their corresponding

https://doi.org/10.1021/acsomega.3c00436
ACS Omega 2023, 8, 13177−13191

operating conditions, components, and compositions based on the reported references. The results are also summarized in Table 4. It can be observed that the predicted densities

Table 4. Summary of the Utilized Database and the Statistical Evaluation Metrics for the Model Developed in this Work Compared to the Haghbakhsh Correlation[72]

	total	binary	ternary
	Database		
DES constituents	180	163	67
distinct DES mixtures	347	260	87
DES compositions	1016	573	334
data points	4995	3553	1442
	Haghbakhsh et al.[72]		
RMSE (g/mL)	0.1143	0.1046	0.1353
ASD (g/mL)	±0.0550	±0.0535	±0.0587
AARD (%)	7.187	7.383	6.704
	This Work		
RMSE (g/mL)	0.0889	0.0776	0.1119
ASD (g/mL)	±0.0435	±0.0417	±0.0478
AARD (%)	5.565	5.712	5.203

demonstrate acceptable deviations from the experimental data with an AARD of 6.704%. Given the good accuracy in predicting the density of the ternary DESs, the results suggest that the presented critical properties and acentric factors of the ternary DESs could be considered as a reliable method to extend models developed for binary DESs to ternary DESs.

To show how the determined critical properties and acentric factors can be used for the development of computational models for ternary DESs, we also developed in this work a similar model that is based on the density of 4995 data points (Table 4), which was established with stepwise regression and analysis of variance (ANOVA) using JMP SAS Pro software (version 16).[73,74] The algorithm resulted in the following expression in eq 19, which is detailed in Table 5.

$$\rho(\mathrm{g/mL}) = -4.717 \times 10^{-7}(T_{c,DES}{}^{2}) + 9.098 \times 10^{-4}(T_{c,DES}) + 7.1965 \times 10^{-2}(\omega_{DES}{}^{0.67131}) - 2.034 \times 10^{-3}(V_{c,DES}) - 6.540 \times 10^{-4}(T) - 6.051 \times 10^{-5}(P_{c,DES}) + 6.1911 \times 10^{-3}(M_{DES}) + 0.8597 \quad (19)$$

As can be observed in Table 5, all of the parameters investigated were observed to be significant from their p-value analysis ($p < 0.05$). The relative importance of each input can be seen from their $|t_{\text{-ratio}}|$ values, where it can be observed that the most influential parameters were $V_{c,DES}$ and M_{DES}, while the least influential parameters were $P_{c,DES}$ and $T^2_{c,DES}$. The performance of the model was also evaluated using various metrics including the root mean squared error (RMSE), average standard deviation (ASD), and AARD. The results are displayed in Table 4 and shown graphically as a bar chart distribution of the relative deviation in Figure 4 for both binary

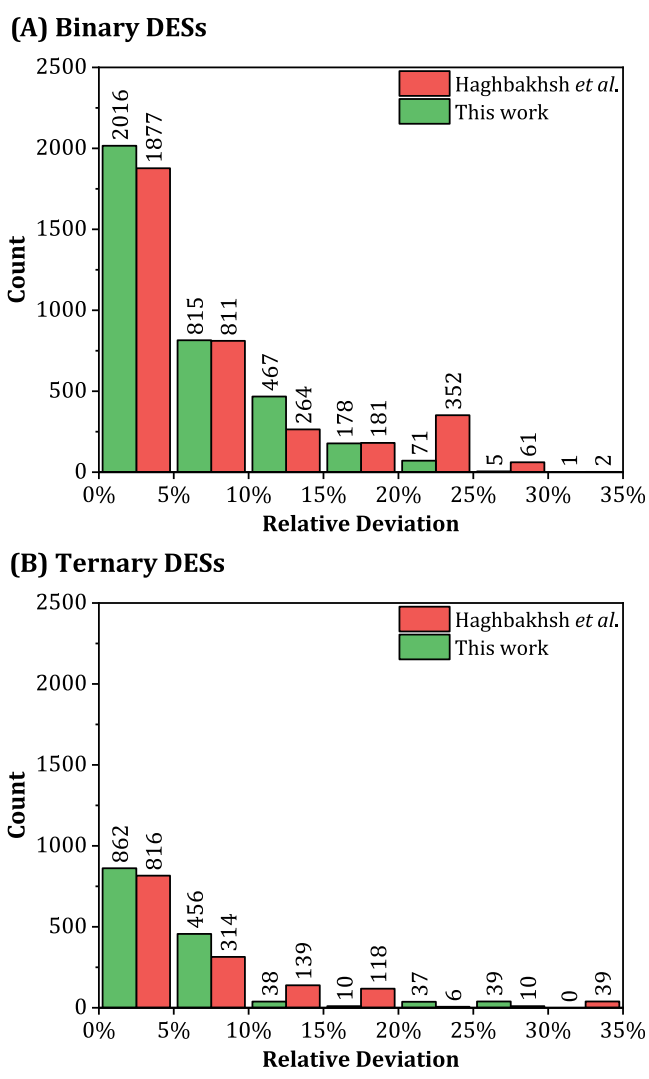

Figure 4. Relative deviation distribution of the experimental and predicted densities for the database of (A) binary and (B) ternary DESs using the Haghbakhsh correlation and the model developed in this work.

Table 5. Analysis of Variance for the Developed Model between the Critical Properties and the Density

variable	coefficient	standard Error	$\lvert t_{\text{-ratio}}\rvert$	95% confidence interval	p-value
$T^2_{c,DES}$	-4.7170×10^{-7}	1.2370×10^{-7}	3.81	$[-4.7789, -4.6552] \times 10^{-7}$	0.0002
$T_{c,DES}$	9.0980×10^{-4}	1.8600×10^{-4}	4.90	$[9.0050, 9.1910] \times 10^{-4}$	<0.0001
$\omega_{DES}^{0.67131}$	7.1965×10^{-2}	9.3080×10^{-3}	7.73	$[7.1499, 7.2430] \times 10^{-2}$	<0.0001
$V_{c,DES}$	-2.0340×10^{-3}	3.0230×10^{-5}	67.27	$[-2.0355, -2.0325] \times 10^{-3}$	<0.0001
T	-6.5400×10^{-4}	6.1000×10^{-5}	10.72	$[-6.5705, -6.5095] \times 10^{-4}$	<0.0001
$P_{c,DES}$	-6.0510×10^{-5}	1.5315×10^{-5}	3.95	$[-6.1276, -5.9744] \times 10^{-5}$	<0.0001
M_{DES}	6.1911×10^{-3}	1.3900×10^{-4}	44.45	$[6.1842, 6.1981] \times 10^{-3}$	<0.0001
intercept	8.5966×10^{-1}	7.0351×10^{-1}	12.22	$[8.5614, 8.6317] \times 10^{-1}$	<0.0001

https://doi.org/10.1021/acsomega.3c00436
ACS Omega 2023, 8, 13177−13191

DESs in (A) and ternary DESs in (B). It can be observed that the model provides predictions that are within a satisfactory accuracy range with RMSE, ASD, and AARD values of 0.0889 g/mL, ±0.0435 g/mL, and 5. 565%, respectively. It can also be observed that it outperformed the correlation reported by Haghbakhsh et al.[72] in predicting both binary and ternary DESs with AARD values of 5.712% compared to 7.383% for binary DESs and 5.203% compared to 6.704% for ternary DESs. The enhanced performance is expected to be due to the bigger data set used for training the model (4,995 data points compared to 1239 points). Moreover, the predictive capabilities of the developed model were showcased by determining the density predictions of ChCl:LA:EG across the compositional range of 20−60 mol%, which is presented in Figure 3.

As aforementioned, the reported framework in this work can extend pre-existing models available in the literature for binary DESs to ternary DESs. For instance, Taherzadeh et al.[75] developed a simple model to predict the refractive indices of binary DESs using 153 DES compositions that achieved an AARD of 1.03%. Furthermore, Haghbakhsh et al.[76] also reported another model to predict the surface tension of binary DESs using 112 DES compositions, and the model's overall AARD was determined to be 8.80%. Other simple models using the modified LJR critical properties and acentric factors as inputs have also been developed for the speed of sound[77] and heat capacity[78] of binary DESs. Ideally, it would be beneficial to evaluate the performance of these developed models for the refractive indices, surface tensions, speeds of sound, and heat capacities of ternary DESs at this stage. However, the lack of literature data on these properties for ternary DESs poses a challenge currently, and thus, they were not tested. Nonetheless, other than the extension of binary DES models, the presented critical properties and acentric factors of the DESs reported herein can also be used to develop new and novel models tailored to both binary and ternary DESs, as demonstrated in this work using eq 19.

4. CONCLUSIONS

In this study, the modified Lydersen−Joback−Reid (LJR) group method was combined with Lee−Kesler mixing rules to determine the critical properties ($V_{c,DES}$, $T_{c,DES}$, $P_{c,DES}$) and acentric factors (ω_{DES}) of 87 distinct ternary deep eutectic solvents (DESs). The approach can be applied to any DES constituent, including the 47 functional groups defined by the modified LJR method. To validate the model, the critical properties and acentric factors were utilized to predict the densities of the ternary DESs. The results showed good agreement between the experimental and predicted data, with an AARD of 5.203% for ternary DESs. Using the framework reported in this work, the previously reported models for binary DESs can be easily extended to ternary DESs, and the development of new computational models for ternary DESs using critical properties can be readily employed.

■ ASSOCIATED CONTENT

Supporting Information

The Supporting Information is available free of charge at https://pubs.acs.org/doi/10.1021/acsomega.3c00436.

Critical property calculator (Table S1), critical properties of DESs (Table S2), ternary diagram data (Table S3), density data set (Table S4), and critical properties of DES constituents (Table S5) (XLSX)

■ AUTHOR INFORMATION

Corresponding Author

Inas M. AlNashef − *Department of Chemical Engineering, Khalifa University of Science and Technology, 127788 Abu Dhabi, United Arab Emirates; Center for Membrane and Advanced Water Technology (CMAT), Khalifa University, 127788 Abu Dhabi, United Arab Emirates; Research and Innovation Center on CO_2 and Hydrogen (RICH Center), Khalifa University of Science and Technology, 127788 Abu Dhabi, United Arab Emirates;* orcid.org/0000-0003-4654-2932; Email: enas.nashef@ku.ac.ae

Authors

Abir Boublia − *Laboratoire de Physico-Chimie des Hauts Polymères (L PC HP), Département de Génie des Procédés, Faculté de Technologie, Université Ferhat Abbas Sétif-1, Sétif 19000, Algeria;* orcid.org/0000-0003-1669-4951

Tarek Lemaoui − *Department of Process Engineering, Faculty of Technology, Ferhat ABBAS University of Setif, Setif 19000, Algeria;* orcid.org/0000-0002-9634-7134

Ghaiath Almustafa − *Department of Chemical Engineering, Khalifa University of Science and Technology, 127788 Abu Dhabi, United Arab Emirates*

Ahmad S. Darwish − *Department of Chemical Engineering, Khalifa University of Science and Technology, 127788 Abu Dhabi, United Arab Emirates*

Yacine Benguerba − *Laboratoire de Biopharmacie Et Pharmacotechnie (LPBT), Ferhat Abbas Setif 1 University, Setif 19000, Algeria;* orcid.org/0000-0002-8251-9724

Fawzi Banat − *Department of Chemical Engineering, Khalifa University of Science and Technology, 127788 Abu Dhabi, United Arab Emirates; Center for Membrane and Advanced Water Technology (CMAT), Khalifa University, 127788 Abu Dhabi, United Arab Emirates; Research and Innovation Center on CO_2 and Hydrogen (RICH Center), Khalifa University of Science and Technology, 127788 Abu Dhabi, United Arab Emirates;* orcid.org/0000-0002-7646-5918

Complete contact information is available at: https://pubs.acs.org/10.1021/acsomega.3c00436

Author Contributions

[▽]A.B. and T.L.: Shared first authorship.

Notes

The authors declare no competing financial interest.

■ ACKNOWLEDGMENTS

The authors are grateful to and acknowledge the generous support of Khalifa University of Science and Technology, Abu Dhabi, United Arab Emirates, and the support of the Process Engineering Department, Faculty of Technology, Ferhat ABBAS University of Setif, Setif, Algeria.

■ REFERENCES

(1) Abbott, A. P.; Capper, G.; Davies, D. L.; Rasheed, R. K.; Tambyrajah, V. Novel Ambient Temperature Ionic Liquids for Zinc and Zinc Alloy Electrodeposition. *Trans. IMF* **2001**, *79*, 204−206.

(2) Zhang, M.; Zhang, X.; Liu, Y.; Wu, K.; Zhu, Y.; Lu, H.; Liang, B. Insights into the Relationships between Physicochemical Properties, Solvent Performance, and Applications of Deep Eutectic Solvents. *Environ. Sci. Pollut. Res.* **2021**, *28*, 35537−35563.

(3) Smith, E. L.; Abbott, A. P.; Ryder, K. S. Deep Eutectic Solvents (DESs) and Their Applications. *Chem. Rev.* **2014**, *114*, 11060−11082.
(4) Liu, Y.; Friesen, J. B.; McAlpine, J. B.; Lankin, D. C.; Chen, S.-N.; Pauli, G. F. Natural Deep Eutectic Solvents: Properties, Applications, and Perspectives. *J. Nat. Prod.* **2018**, *81*, 679−690.
(5) Hansen, B. B.; Spittle, S.; Chen, B.; Poe, D.; Zhang, Y.; Klein, J. M.; Horton, A.; Adhikari, L.; Zelovich, T.; Doherty, B. W.; et al. Deep Eutectic Solvents: A Review of Fundamentals and Applications. *Chem. Rev.* **2021**, *121*, 1232−1285.
(6) El Achkar, T.; Greige-Gerges, H.; Fourmentin, S. Basics and Properties of Deep Eutectic Solvents: A Review. *Environ. Chem. Lett.* **2021**, *19*, 3397−3408.
(7) Wang, X.; Jiang, W.; Zhu, W.; Li, H.; Yin, S.; Chang, Y.; Li, H. A Simple and Cost-Effective Extractive Desulfurization Process with Novel Deep Eutectic Solvents. *RSC Adv.* **2016**, *6*, 30345−30352.
(8) Van Osch, D. J. G. P.; Zubeir, L. F.; Van Den Bruinhorst, A.; Rocha, M. A. A.; Kroon, M. C. Hydrophobic Deep Eutectic Solvents as Water-Immiscible Extractants. *Green Chem.* **2015**, *17*, 4518−4521.
(9) Greaves, T. L.; Drummond, C. J. Protic Ionic Liquids: Properties and Applications. *Chem. Rev.* **2008**, *108*, 206−237.
(10) Zeng, C.-X.; Qi, S.-J.; Xin, R.-P.; Yang, B.; Wang, Y.-H. Synergistic Behavior of Betaine−Urea Mixture: Formation of Deep Eutectic Solvent. *J. Mol. Liq.* **2016**, *219*, 74−78.
(11) Ijardar, S. P.; Singh, V.; Gardas, R. L. Revisiting the Physicochemical Properties and Applications of Deep Eutectic Solvents. *Molecules* **2022**, *27*, No. 1368.
(12) Lemaoui, T.; Boublia, A.; Darwish, A. S.; Alam, M.; Park, S.; Jeon, B.-H.; Banat, F.; Benguerba, Y.; AlNashef, I. M. Predicting the Surface Tension of Deep Eutectic Solvents Using Artificial Neural Networks. *ACS Omega* **2022**, *7*, 32194−32207.
(13) Boublia, A.; Lemaoui, T.; Abu Hatab, F.; Darwish, A. S.; Banat, F.; Benguerba, Y.; AlNashef, I. M. Molecular-Based Artificial Neural Network for Predicting the Electrical Conductivity of Deep Eutectic Solvents. *J. Mol. Liq.* **2022**, *366*, No. 120225.
(14) Lemaoui, T.; Abu Hatab, F.; Darwish, A. S.; Attoui, A.; Hammoudi, N. E. H.; Almustafa, G.; Benaicha, M.; Benguerba, Y.; Alnashef, I. M. Molecular-Based Guide to Predict the PH of Eutectic Solvents: Promoting an Efficient Design Approach for New Green Solvents. *ACS Sustainable Chem. Eng.* **2021**, *9*, 5783−5808.
(15) Almustafa, G.; Darwish, A. S.; Lemaoui, T.; O'Conner, M. J.; Amin, S.; Arafat, H. A.; AlNashef, I. Liquification of 2,2,4-Trimethyl-1,3-Pentanediol into Hydrophobic Eutectic Mixtures: A Multi-Criteria Design for Eco-Efficient Boron Recovery. *Chem. Eng. J.* **2021**, *426*, No. 131342.
(16) Halder, A. K.; Haghbakhsh, R.; Voroshylova, I. V.; Duarte, A. R. C.; Cordeiro, M. N. D. S. Density of Deep Eutectic Solvents: The Path Forward Cheminformatics-Driven Reliable Predictions for Mixtures. *Molecules* **2021**, *26*, No. 5779.
(17) Verónica, A.; Cecília, C.; Biswas, A.; Buttrum, M.; Kim, S.; Boddu, V. M.; Cheng, H. N. LWT - Food Science and Technology Microwave-Assisted Extraction of Soluble Sugars from Banana Puree with Natural Deep Eutectic Solvents (NADES). *LWT* **2019**, *107*, 79−88.
(18) Lemaoui, T.; Darwish, A. S.; Attoui, A.; Abu Hatab, F.; Hammoudi, N. E. H.; Benguerba, Y.; Vega, L. F.; Alnashef, I. M. Predicting the Density and Viscosity of Hydrophobic Eutectic Solvents: Towards the Development of Sustainable Solvents. *Green Chem.* **2020**, *22*, 8511−8530.
(19) Nowosielski, B.; Jamrógiewicz, M.; Łuczak, J.; Warmińska, D. Novel Binary Mixtures of Alkanolamine Based Deep Eutectic Solvents with Water—Thermodynamic Calculation and Correlation of Crucial Physicochemical Properties. *Molecules* **2022**, *27*, No. 788.
(20) Smith, P. J.; Arroyo, C. B.; Hernandez, F. L.; Goeltz, J. C. Ternary Deep Eutectic Solvent Behavior of Water and Urea − Choline Chloride Mixtures. *J. Phys. Chem. B* **2019**, *123*, 5302−5306.
(21) Lei, Z.; Zhang, J.; Li, Q.; Chen, B. UNIFAC Model for Ionic Liquids. *Ind. Eng. Chem. Res.* **2009**, *48*, 2697−2704.
(22) Hizaddin, H. F.; Hadj-Kali, M. K.; Alnashef, I. M.; Mjalli, F. S.; Hashim, M. A. Prediction of CO2 Solubility in Ionic Liquids Using the PSRK Model. *J. Supercrit. Fluids* **2015**, *100*, 184−193.
(23) Darwish, A. S.; Abu Hatab, F.; Lemaoui, T.; A Z Ibrahim, O.; Almustafa, G.; Zhuman, B.; E E Warrag, S.; Hadj-Kali, M. K.; Benguerba, Y.; Alnashef, I. M. Multicomponent Extraction of Aromatics and Heteroaromatics from Diesel Using Acidic Eutectic Solvents: Experimental and COSMO-RS Predictions. *J. Mol. Liq.* **2021**, *336*, No. 116575.
(24) Valderrama, J. O.; Alvarez, V. H. A New Group Contribution Method Based on Equation of State Parameters to Evaluate the Critical Properties of Simple and Complex Molecules. *Can. J. Chem. Eng.* **2008**, *84*, 431−446.
(25) Valderrama, J. O.; Forero, L. A.; Rojas, R. E. Critical Properties and Normal Boiling Temperature of Ionic Liquids. Update and a New Consistency Test. *Ind. Eng. Chem. Res.* **2012**, *51*, 7838−7844.
(26) Valderrama, J. O.; Forero, L. A.; Rojas, R. E. Critical Properties of Metal-Containing Ionic Liquids. *Ind. Eng. Chem. Res.* **2019**, *58*, 7332−7340.
(27) Valderrama, J. O.; Robles, P. A. Critical Properties, Normal Boiling Temperatures, and Acentric Factors of Fifty Ionic Liquids. *Ind. Eng. Chem. Res.* **2007**, *46*, 1338−1344.
(28) Mirza, N. R.; Nicholas, N. J.; Wu, Y.; Kentish, S.; Stevens, W. Estimation of Normal Boiling Temperatures, Critical Properties, and Acentric Factors of Deep Eutectic Solvents. *J. Chem. Eng. Data* **2015**, *60*, 1844−1854.
(29) Adeyemi, I.; Abu-Zahra, M. R. M.; AlNashef, I. M. Physicochemical Properties of Alkanolamine-Choline Chloride Deep Eutectic Solvents: Measurements, Group Contribution and Artificial Intelligence Prediction Techniques. *J. Mol. Liq.* **2018**, *256*, 581−590.
(30) Almustafa, G.; Sulaiman, R.; Kumar, M.; Adeyemi, I.; Arafat, H. A.; AlNashef, I. Boron Extraction from Aqueous Medium Using Novel Hydrophobic Deep Eutectic Solvents. *Chem. Eng. J.* **2020**, *395*, No. 125173.
(31) Knapp, H.; Doring, R.; Oellrich, L.; Plocker, U.; Prausnitz, J. M. *Vapour−Liquid Equilibria for Mixtures of Low Boiling Substances*; DECHEMA: Frankfurt, 1982; Vol. *5*.
(32) Plocker, U.; Knapp, H.; Prausnitz, J. Calculation of High-Pressure Vapor-Liquid Equilibria from a Corresponding-States Correlation with Emphasis on Asymmetric Mixtures. *Ind. Eng. Chem. Process Des. Dev.* **1978**, *17*, 324−332.
(33) García, C. B.; García, J.; Martín, M. M. L.; Salmerón, R. Collinearity: Revisiting the Variance Inflation Factor in Ridge Regression. *J. Appl. Stat.* **2015**, *42*, 648−661.
(34) Tao, D.; Qu, F.; Li, Z.; Zhou, Y. Promoted Absorption of CO at High Temperature by Cuprous-Based Ternary Deep Eutectic Solvents. *AIChE J.* **2021**, *67*, No. e17106.
(35) Gómez, A. V.; Tadini, C. C.; Biswas, A.; Buttrum, M.; Kim, S.; Boddu, V. M.; Cheng, H. N. Microwave-Assisted Extraction of Soluble Sugars from Banana Puree with Natural Deep Eutectic Solvents (NADES). *LWT* **2019**, *107*, 79−88.
(36) Ghaedi, H.; Ayoub, M.; Sufian, S.; Shariff, A. M.; Murshid, G.; Hailegiorgis, S. M.; Khan, S. N. Density, Excess and Limiting Properties of (Water and Deep Eutectic Solvent) Systems at Temperatures from 293.15 K to 343.15 K. *J. Mol. Liq.* **2017**, *248*, 378−390.
(37) Taysun, M. B.; Sert, E.; Atalay, F. S. Effect of Hydrogen Bond Donor on the Physical Properties of Benzyltriethylammonium Chloride Based Deep Eutectic Solvents and Their Usage in 2-Ethyl-Hexyl Acetate Synthesis as a Catalyst. *J. Chem. Eng. Data* **2017**, *62*, 1173−1181.
(38) Taysun, M. B.; Sert, E.; Atalay, F. S. Physical Properties of Benzyl Tri-Methyl Ammonium Chloride Based Deep Eutectic Solvents and Employment as Catalyst. *J. Mol. Liq.* **2016**, *223*, 845−852.
(39) Cardellini, F.; Tiecco, M.; Germani, R.; Cardinali, G.; Corte, L.; Roscini, L.; Spreti, N. Novel Zwitterionic Deep Eutectic Solvents from Trimethylglycine and Carboxylic Acids: Characterization of

https://doi.org/10.1021/acsomega.3c00436
ACS Omega 2023, 8, 13177−13191

Their Properties and Their Toxicity. *RSC Adv.* **2014**, *4*, 55990−56002.
(40) Zhao, B.-Y.; Xu, P.; Yang, F.-X.; Wu, H.; Zong, M.-H.; Lou, W.-Y. Biocompatible Deep Eutectic Solvents Based on Choline Chloride: Characterization and Application to the Extraction of Rutin from Sophora Japonica. *ACS Sustainable Chem. Eng.* **2015**, *3*, 2746−2755.
(41) Leron, R. B.; Soriano, A. N.; Li, M.-H. Densities and Refractive Indices of the Deep Eutectic Solvents (Choline Chloride + Ethylene Glycol or Glycerol) and Their Aqueous Mixtures at the Temperature Ranging from 298.15 to 333.15 K. *J. Taiwan Inst. Chem. Eng.* **2012**, *43*, 551−557.
(42) Seyf, J. Y.; Zarei, F. Density, Viscosity, and Refractive Index of a Choline Chloride + <scp>d</Scp> -(−)-Fructose Deep Eutectic Solvent + Water Mixture at Different Temperatures: An Experimental Study and Thermodynamic Modeling. *J. Chem. Eng. Data* **2022**, *67*, 3007−3021.
(43) Silva, L. P.; Fernandez, L.; Conceição, J. H. F.; Martins, M. A. R.; Sosa, A.; Ortega, J.; Pinho, S. P.; Coutinho, J. A. P. Design and Characterization of Sugar-Based Deep Eutectic Solvents Using Conductor-like Screening Model for Real Solvents. *ACS Sustainable Chem. Eng.* **2018**, *6*, 10724−10734.
(44) Mjalli, F. S.; Ahmad, O. Density of Aqueous Choline Chloride-Based Ionic Liquids Analogues. *Thermochim. Acta* **2017**, *647*, 8−14.
(45) Moghimi, M.; Roosta, A. Physical Properties of Aqueous Mixtures of (Choline Chloride + Glucose) Deep Eutectic Solvents. *J. Chem. Thermodyn.* **2019**, *129*, 159−165.
(46) Yadav, A.; Kar, J. R.; Verma, M.; Naqvi, S.; Pandey, S. Densities of Aqueous Mixtures of (Choline Chloride+ethylene Glycol) and (Choline Chloride+malonic Acid) Deep Eutectic Solvents in Temperature Range 283.15−363.15K. *Thermochim. Acta* **2015**, *600*, 95−101.
(47) Rodriguez Rodriguez, N.; Machiels, L.; Binnemans, K. P -Toluenesulfonic Acid-Based Deep-Eutectic Solvents for Solubilizing Metal Oxides. *ACS Sustainable Chem. Eng.* **2019**, *7*, 3940−3948.
(48) Yadav, A.; Pandey, S. Densities and Viscosities of (Choline Chloride + Urea) Deep Eutectic Solvent and Its Aqueous Mixtures in the Temperature Range 293.15 K to 363.15 K. *J. Chem. Eng. Data* **2014**, *59*, 2221−2229.
(49) Moradi, K.; Rahimi, S.; Ebrahimi, S.; Salimi, A. Understanding the Bulk and Interfacial Structures of Ternary and Binary Deep Eutectic Solvents with a Constant Potential Method: A Molecular Dynamics Study. *Phys. Chem. Chem. Phys.* **2022**, *24*, 10962−10973.
(50) Liu, Y.-T.; Chen, Y.-A.; Xing, Y.-J. Synthesis and Characterization of Novel Ternary Deep Eutectic Solvents. *Chin. Chem. Lett.* **2014**, *25*, 104−106.
(51) Faraji, M.; Noormohammadi, F.; Adeli, M. Preparation of a Ternary Deep Eutectic Solvent as Extraction Solvent for Dispersive Liquid-Liquid Microextraction of Nitrophenols in Water Samples. *J. Environ. Chem. Eng.* **2020**, *8*, No. 103948.
(52) Subba, N.; Sahu, P.; Das, N.; Sen, P. Rational Design, Preparation and Characterization of a Ternary Non-Ionic Room-Temperature Deep Eutectic Solvent Derived from Urea, Acetamide, and Sorbitol. *J. Chem. Sci.* **2021**, *133*, No. 25.
(53) Wang, Q.; Wang, Y.; Sun, X.; Wei, L.; Wei, L.; Zhai, S.; Xiao, Z.; An, Q.; Hao, J. Constructing Ternary Deep Eutectic Solvents with Multiple Sites for Ammonia Storage. *Int. J. Hydrogen Energy* **2022**, *47*, 34102−34111.
(54) Saei, A.; Javadi, A.; Afshar Mogaddam, M. R.; Mirzaei, H.; Nemati, M. Development of Homogeneous Liquid−Liquid Extraction Combined with Dispersive Liquid−Liquid Microextraction Based on Solidification of Floating Droplets of a Ternary Component Deep Eutectic Solvent for the Analysis of Antibiotic Residues in Sausage Samples. *Anal. Methods* **2020**, *12*, 4220−4228.
(55) Alavinia, S.; Ghorbani-Vaghei, R. Magnetic Fe3O4 Nanoparticles in Melamine-Based Ternary Deep Eutectic Solvent as a Novel Eco-Compatible System for Green Synthesis of Pyrido[2,3-d]Pyrimidine Derivatives. *J. Mol. Struct.* **2022**, *1270*, No. 133860.
(56) Jablonsky, M.; Majova, V.; Ondrigova, K.; Sima, J. Preparation and Characterization of Physicochemical Properties and Application of Novel Ternary Deep Eutectic Solvents. *Cellulose* **2019**, *26*, 3031−3045.
(57) Majová, V.; Jablonský, M.; Lelovský, M. Delignification of Unbleached Pulp by Ternary Deep Eutectic Solvents. *Green Process. Synth.* **2021**, *10*, 666−676.
(58) K, S. Synthesis and Characterization of Silver Nanoparticles Using Zinc Chloride-Sugar-Amino Acids Based Novel Ternary Deep Eutectic Solvents. *ECS Trans.* **2022**, *107*, 4113−4127.
(59) Wang, J.; Baker, S. N. Pyrrolidinium Salt Based Binary and Ternary Deep Eutectic Solvents: Green Preparations and Physiochemical Property Characterizations. *Green Process. Synth.* **2018**, *7*, 353−359.
(60) Kadhom, M. A.; Abdullah, G. H.; Al-Bayati, N. Studying Two Series of Ternary Deep Eutectic Solvents (Choline Chloride−Urea−Glycerol) and (Choline Chloride−Malic Acid−Glycerol), Synthesis and Characterizations. *Arab. J. Sci. Eng.* **2017**, *42*, 1579−1589.
(61) Tang, W.; Li, G.; Chen, B.; Zhu, T.; Row, K. H. Evaluating Ternary Deep Eutectic Solvents as Novel Media for Extraction of Flavonoids from Ginkgo Biloba. *Sep. Sci. Technol.* **2017**, *52*, 91−99.
(62) Atri, R. S.; Sanchez-Fernandez, A.; Hammond, O. S.; Manasi, I.; Doutch, J.; Tellam, J. P.; Edler, K. J. Morphology Modulation of Ionic Surfactant Micelles in Ternary Deep Eutectic Solvents. *J. Phys. Chem. B* **2020**, *124*, 6004−6014.
(63) Saputra, R.; Walvekar, R.; Khalid, M.; Mubarak, N. M. Synthesis and Thermophysical Properties of Ethylammonium Chloride-Glycerol-ZnCl2 Ternary Deep Eutectic Solvent. *J. Mol. Liq.* **2020**, *310*, No. 113232.
(64) Zhu, Q.; Wang, C.; Yin, J.; Li, H.; Jiang, W.; Liu, J.; Li, P.; Zhang, Q.; Chen, Z.; Zhu, W. Efficient and Remarkable SO2 Capture: A Discovery of Imidazole-Based Ternary Deep Eutectic Solvents. *J. Mol. Liq.* **2021**, *330*, No. 115595.
(65) Zhong, F.-Y.; Zhou, L.; Shen, J.; Liu, Y.; Fan, J.-P.; Huang, K. Rational Design of Azole-Based Deep Eutectic Solvents for Highly Efficient and Reversible Capture of Ammonia. *ACS Sustainable Chem. Eng.* **2019**, *7*, 14170−14179.
(66) Zhong, F.-Y.; Peng, H.-L.; Tao, D.-J.; Wu, P.-K.; Fan, J.-P.; Huang, K. Phenol-Based Ternary Deep Eutectic Solvents for Highly Efficient and Reversible Absorption of NH 3. *ACS Sustainable Chem. Eng.* **2019**, *7*, 3258−3266.
(67) Wang, C.; Bi, Q.; Huo, Y.; Zhang, Z.; Tao, D.; Shen, Y.; Zhu, Q.; Chen, Z.; Li, H.; Zhu, W. Investigation of Amine-Based Ternary Deep Eutectic Solvents for Efficient, Rapid, and Reversible SO 2 Absorption. *Energy Fuels* **2021**, *35*, 20406−20410.
(68) Cui, G.; Jiang, K.; Liu, H.; Zhou, Y.; Zhang, Z.; Zhang, R.; Lu, H. Highly Efficient CO Removal by Active Cuprous-Based Ternary Deep Eutectic Solvents [HDEEA][Cl] + CuCl + EG. *Sep. Purif. Technol.* **2021**, *274*, No. 118985.
(69) Warrag, S. E. E.; Darwish, A. S.; Adeyemi, I. A.; Hadj-Kali, M. K.; Kroon, M. C.; Alnashef, I. M. Extraction of Pyridine from N-Alkane Mixtures Using Methyltriphenylphosphonium Bromide-Based Deep Eutectic Solvents as Extractive Denitrogenation Agents. *Fluid Phase Equilib.* **2020**, *517*, No. 112622.
(70) Haider, M. B.; Jha, D.; Kumar, R.; Marriyappan Sivagnanam, B. Ternary Hydrophobic Deep Eutectic Solvents for Carbon Dioxide Absorption. *Int. J. Greenhouse Gas Control* **2020**, *92*, No. 102839.
(71) Chemat, F.; Anjum, H.; Shariff, A. M.; Kumar, P.; Murugesan, T. Thermal and Physical Properties of (Choline Chloride + Urea +l-Arginine) Deep Eutectic Solvents. *J. Mol. Liq.* **2016**, *218*, 301−308.
(72) Haghbakhsh, R.; Bardool, R.; Bakhtyari, A.; Duarte, A. R. C.; Raeissi, S. Simple and Global Correlation for the Densities of Deep Eutectic Solvents. *J. Mol. Liq.* **2019**, *296*, No. 111830.
(73) Lemaoui, T.; Darwish, A. S.; Hammoudi, N. E. H.; Abu Hatab, F.; Attoui, A.; Alnashef, I. M.; Benguerba, Y. Prediction of Electrical Conductivity of Deep Eutectic Solvents Using COSMO-RS Sigma Profiles as Molecular Descriptors: A Quantitative Structure−Property Relationship Study. *Ind. Eng. Chem. Res.* **2020**, *59*, 13343−13354.
(74) Lemaoui, T.; Darwish, A. S.; Attoui, A.; Hatab, F. A.; El, N.; Hammoudi, H.; Benguerba, Y.; Vega, L. F.; Alnashef, I. M. Predicting the Density and Viscosity of Hydrophobic Eutectic Solvents: Towards

https://doi.org/10.1021/acsomega.3c00436
ACS Omega 2023, 8, 13177−13191

the Development of Sustainable Solvents †. *Green Chem.* **2020**, *22*, 8511−8530.
(75) Taherzadeh, M.; Haghbakhsh, R.; Duarte, A. R. C.; Raeissi, S. Generalized Model to Estimate the Refractive Indices of Deep Eutectic Solvents. *J. Chem. Eng. Data* **2020**, *65*, 3965−3976.
(76) Haghbakhsh, R.; Taherzadeh, M.; Duarte, A. R. C.; Raeissi, S. A General Model for the Surface Tensions of Deep Eutectic Solvents. *J. Mol. Liq.* **2020**, *307*, No. 112972.
(77) Peyrovedin, H.; Haghbakhsh, R.; Duarte, A. R. C.; Raeissi, S. A Global Model for the Estimation of Speeds of Sound in Deep Eutectic Solvents. *Molecules* **2020**, *25*, No. 1626.
(78) Taherzadeh, M.; Haghbakhsh, R.; Duarte, A. R. C.; Raeissi, S. Estimation of the Heat Capacities of Deep Eutectic Solvents. *J. Mol. Liq.* **2020**, *307*, No. 112940.

https://doi.org/10.1021/acsomega.3c00436
ACS Omega 2023, 8, 13177−13191